

DETECTION OF OIL PRODUCT ON THE WATER SURFACE WITH THERMAL INFRARED CAMERA

Kristina PILŽIS¹, Vaidotas VAIŠIS²

Vilnius Gediminas Technical University, Vilnius, Lithuania
E-mails: ¹kristina.pilzis@stud.vgtu.lt; ²vaidotas.vaisis@vgtu.lt

Abstract. From all existing remote detectors infrared sensors are the cheapest and most widely used. In this article described experiment was done to determine if it is possible to detected oil products on the water surface using thermal infrared camera. This hypothesis was confirmed – thickest layer of used oil product appeared hotter than water. Also, it was found that temperatures of oil product on the surface directly depend on the air temperature. However, clouds have a significant effect on efficiency of this remote sensing method.

Keywords: oil spill, water surface, remote sensing, infrared sensors, thermal infrared camera.

Introduction

Crude oil floating on ocean surfaces can harm marine and coastal environments as well as fisheries and tourism (Leifer *et al.* 2012). Hazardous substances present in crude oil can be transferred from aquatic organisms such as phytoplankton to higher levels of the food chain, leading to the loss of eggs or even death for oiled birds (Jha *et al.* 2008).

For a spill on open water, the oil spreads into a relatively thin slick on the surface. The thickness of the slick depends on the type of oil, with heavy oils forming thicker slicks (on the order of a few millimeters). The movement and thinning of the slick are affected by sea state with the oil being moved along the surface by the surface currents and wind (Fingas 2011).

Weathering processes such as evaporation, water-in-oil emulsification and natural dispersion in the water column are subject to environmental conditions, such as temperature and sea state, as well as the physical properties of the released oil. Weathering of an open water spill can greatly reduce the effectiveness of spill clean-up countermeasures, making it crucial that countermeasures be deployed quickly before the oil emulsifies (Puestow *et al.* 2013). This is why timely and accurate detection of surface oil is important for the monitoring of oil spills and the management of marine and coastal resources (Leifer *et al.* 2012).

Various remote sensing technologies have been used to detect oil slicks, from laser fluorosensors, optical remote sensing (ultraviolet and others) till microwave sensors. However, the most widely used and the cheapest one are

infrared sensors form optical remote sensing (Fingas, Brown 2000). This remote sensing method refers to the fact that in daytime oil absorbs light and emits this as thermal energy at temperatures 3 to 8 K above ambient, primarily in the 8 to 14 μm region. This is detectable by infrared (IR) cameras (Fingas 2015). The main task of this work was to determine the efficiency and applicability of infrared remote sensing method.

Methodology

The experiment was conducted outdoors during a sunny day with sometimes passing small clouds using the experimental settings as shown in the figure 1. In experiment a container with water was used and different thickness layers of oil products using 6 small transparent plastic rings were formed. Inside the rings were created layers with

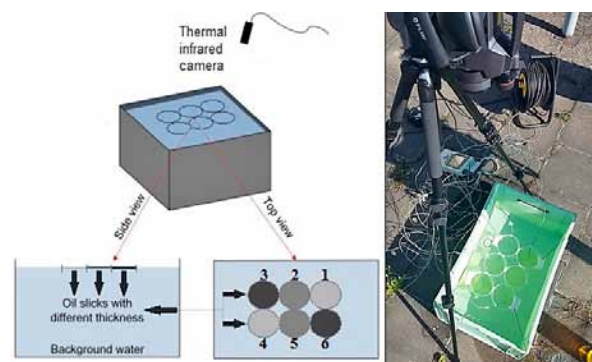


Fig. 1. Diesel detection using infrared camera

1 pav. Dyzelino aptikimas naudojant infraudonųjų spindulių kamerą



Fig. 2. a) ALMEMO® sensor; b) ALMEMO® connector; c) FLIR camera

2 pav. ALMEMO® sensorius (a); ALMEMO® jungtis (b); FLIR kamera (c)

3 different thicknesses (2 rings for the layers of the same thickness). Plastic foam was used to maintain plastic rings on the water surface. As an oil product diesel was used.

Experiment lasted almost 4 hours (from 08:57 till 12:43) and parameters were measured every 20 seconds. In the end were obtained temperature data of 680 measurements. Some of the measured parameters were air and water temperatures, also temperatures of diesel layers in each circle. In total were obtained 8 parameters of temperature. All temperatures were measured using thermocouples, which were connected to the ALMEMO® 2890-9 sensor (Fig. 2 a)) using ALMEMO® ZA 9020-FS Thermo E4 connectors (Fig. 2 b)). 2nd and 3rd channels of thermocouples were representing the temperatures of the thinnest layers of diesel (in 1st and 4th rings of 1 mm thickness), 1st and 4th – medium thickness (2nd and 5th rings of 2 mm thickness), and 0 and 5th – thickest layers of diesel (3rd and 6th rings of 3 mm thickness), as is shown in the figure 2.1. 6th channel was for air, and 7th – for water temperatures. Also, at the same time were taken pictures using FLIR B660 thermal camera (Fig. 2 c)) and digital camera. In total were taken 1360 pictures – half with FLIR and half with digital camera.

Obtained photos were processed using FLIR Tools program changing colour scales of temperatures in order to obtain visual differences between the layers. All data with temperatures were processed and presented using Microsoft Excel program.

Results

In experiment were obtained temperatures of air, water and 6 layers with 3 different thicknesses of diesel (2 measurements for the same thickness). Variations of air and water temperatures are presented in the figure 3.

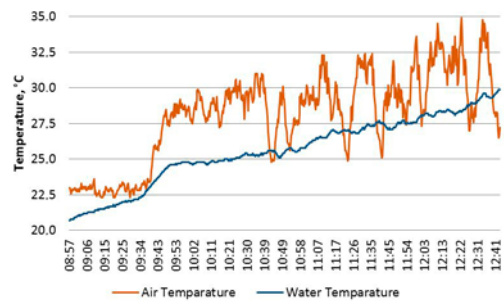


Fig. 3. Variations of water and air temperatures during all experiment

3 pav. Vandens ir oro temperatūrų kitimas eksperimento metu

From the figure 3 can be seen that temperature of water was consistently increasing during experiment. Supposedly, it was increasing due to the rising air temperature. However, it can also be related with the used container, which could heat the water inside it by absorbing direct sun light. Significant fluctuations in air temperature were related with the direct sunlight access: air temperature was decreasing when the clouds have been appearing, in this way sunlight access to the surface has been limited. Air temperature was again increasing only 1–2 minutes after appearance of direct sunlight.

As can be seen from the graphics below (Fig 4, Fig. 5, Fig. 6), temperatures of the diesel layers were directly dependent on air temperature. After about one hour and 40 minutes from the beginning of the experiment temperature of air and the thickest layers of diesel coincided and fluctuations took place at the same time. With the medium layer of diesel thickness it happened after about 1 hour and 45 minutes, and with thinnest layer – hour and a half. Also, it should be mentioned that layers with diesel in the graphs below, which are shown in the red lines, represents layers in the 1st, 2nd and 3rd rings (Fig. 1). These layers in the beginning of the experiment were in the shadow of the container. It could have a significant effect on the temperatures of these layers, because they were increasing slower than of the layers, which during all experiment were under direct sunlight. However, because of the clouds all layers of the diesel sometimes were in the shadow and decrease in the temperatures of these layers was the consequence of absence of direct sunlight. Temperatures of diesel layers in this case coincided with the air temperature changes, as can be seen from the figures 4, 5 and 6.

Also, were compared temperatures of the diesel layers in the 1st, 2nd and the 3rd rings with three different thicknesses, which in the beginning of the experiment were in the shadow (Fig. 7), and temperatures of layers with a different thicknesses of diesel in the 4th, 5th and 6th circles, which were not overlapped by container and did not stay in the shadow (Fig. 8).

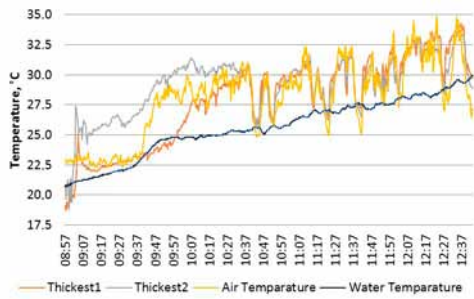


Fig. 4. Temperatures of air, water and the thickest layers of diesel

4 pav. Oro, vandens ir storiausių dyzelio sluoksnių temperatūros

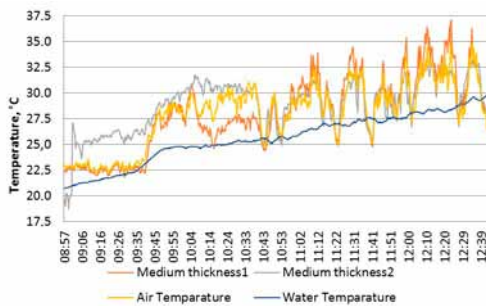


Fig. 5. Temperatures of air, water and the layers with a medium thickness of diesel

5 pav. Oro, vandens ir vidutinio storio dyzelių sluoksnių temperatūros

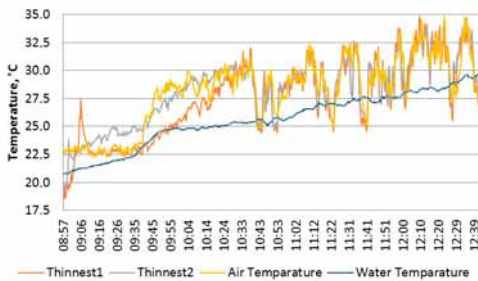


Fig. 6. Temperatures of air, water and the thinnest layers of diesel

6 pav. Oro, vandens ir ploniausių dyzelių sluoksnių temperatūros

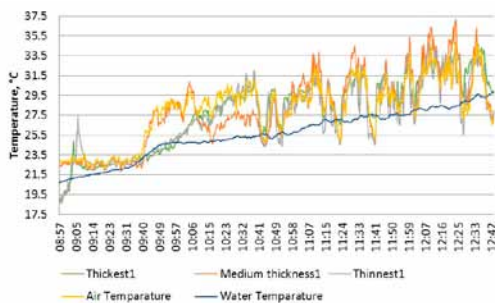


Fig. 7. Temperatures of air, water and diesel layers under shadow in the beginning of the experiment

7 pav. Oro, vandens ir dyzelio sluoksnių, kurie eksperimento pradžioje buvo šešėlyje, temperatūros

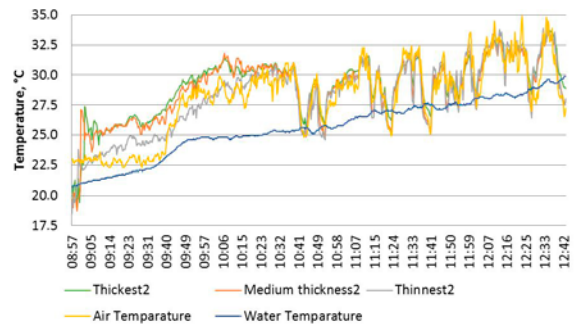


Fig. 8. Temperatures of air, water and diesel layers without shadow

8 pav. Oro, vandens ir dyzelio sluoksnių, kurie viso eksperimento metu nebuvo šešėlyje, temperatūros

It can be concluded, that temperatures of diesel layers, which were not affected by the shadow of the container, correlated with air temperatures more than layers at the shadow. What is more, temperatures of the diesel layers, also as air temperature, were directly affected by the clouds or, in other words, by direct sunlight presence. Without direct sunlight air temperature and temperatures of diesel layers were sometimes even lower than water temperature. Also, temperatures of the thickest layers of diesel after periods exposed with a shadow from the clouds were increasing faster than in the thinnest layers of diesel.

As was mentioned before, at the same time, every 20 seconds, were taken photos of the container with different thickness of diesel layers with infrared FLIR camera and digital camera. In total were taken 1360 pictures, however were chosen 16 of them (8 taken with FLIR camera and 9 with digital camera, in parallel by two), taken every half an hour for the evaluation of differences. Pictures are presented below.

In the figure 9 on the left side can be seen a clear difference between the layers with a different thickness, and rings in the first row shows the difference even more clear. However, as is shown in the photo on the right, that row was in the shadow. It could happen during the time when an equipment was set.

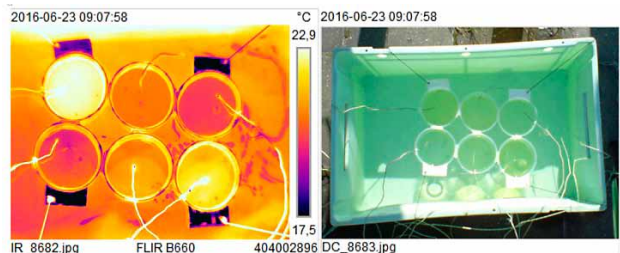


Fig. 9. Infrared (left) and digital (right) photos in the beginning of the experiment

9 pav. Infraraudonųjų spindulių (kairė) ir skaitmeninė (dešinė) nuotraukos eksperimento pradžioje

After half an hour first row of the layers with different diesel thicknesses was in the shadow and infrared photo showed appropriate results (Fig. 10). The temperatures of thickest and medium thickness diesel layers were even lower than temperature of the water that was surrounding them. Quite different results are seen in the second row, which was affected by direct sunlight. The biggest difference can be seen of the thickest layer and not significant difference of thinnest layer.

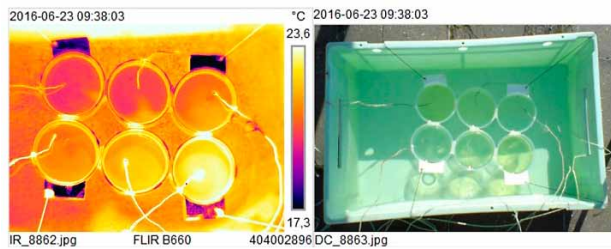


Fig. 10. Infrared (left) and digital (right) photos after half an hour from the beginning of the experiment

10 pav. Infraraudonųjų spindulių (kairė) ir skaitmeninė (dešinė) nuotraukos po pusės valandos nuo eksperimento pradžios

After an hour results of infrared photo were quite similar to the results of the photo taken after half an hour from the beginning of the experiment (Fig. 11). However, the differences between the thickest and medium thickness diesel layer under direct sunlight (second row) and water are more noticeable. In the both thinnest layers of the diesel temperatures according the infrared photo shown in the figure 11 are similar to the water temperature.

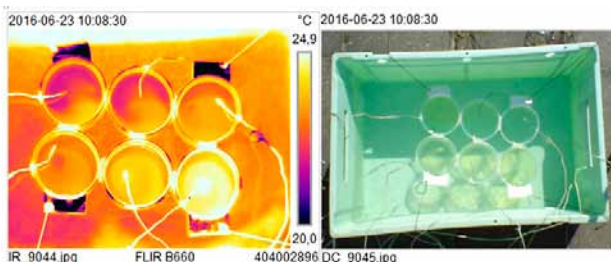


Fig. 11. Infrared (left) and digital (right) photos after an hour from the beginning of the experiment

11 pav. Infraraudonųjų spindulių (kairė) ir skaitmeninė (dešinė) nuotraukos po valandos nuo eksperimento pradžios

As can be seen from the figure 12, differences between the layers in the second row are clear, and temperature of the water is much lower, even in comparison with the thinnest layer of the diesel. First row of the layers is not still fully exposed to direct sunlight; however, the difference in comparison with water temperature is already noticeable.

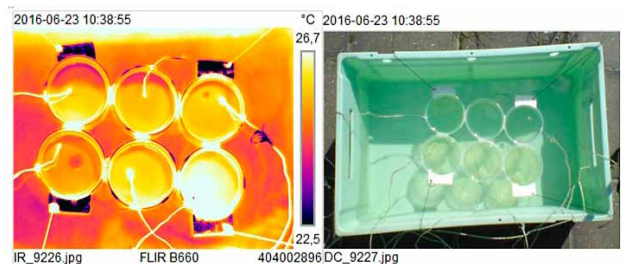


Fig. 12. Infrared (left) and digital (right) photos after hour and a half from the beginning of the experiment

12 pav. Infraraudonųjų spindulių (kairė) ir skaitmeninė (dešinė) nuotraukos po pusantros valandos nuo eksperimento pradžios

An obvious and complete visible difference between the temperature of the water and all layers is seen in the figure 13 on the left. All layers are fully exposed to direct sunlight and the biggest temperatures are seen in the thickest layers of the diesel. The temperature of the layer with a medium diesel thickness in the second row is close to the temperatures of both thickest layers, likely due to a permanent direct solar access.

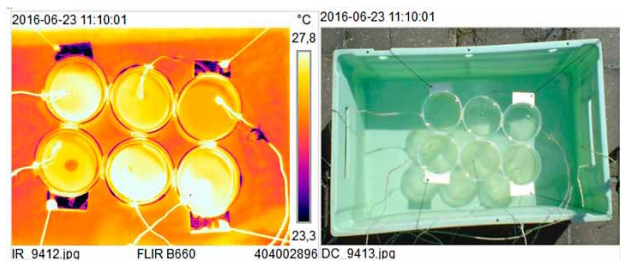


Fig. 13. Infrared (left) and digital (right) photos after two hours from the beginning of the experiment

13 pav. Infraraudonųjų spindulių (kairė) ir skaitmeninė (dešinė) nuotraukos po 2 valandų nuo eksperimento pradžios

Example of an effect of the cloud on the infrared photo is shown in the figure 14. Even if in the photo on the right is shown that there is no shadow, in the figures 3.2–3.6 can be seen, that during this time temperatures of all layers with diesel, also air temperature, were lower because of the shadow, and, as was mentioned before, temperatures after the period with a shadow were increasing during 1–2 minutes.

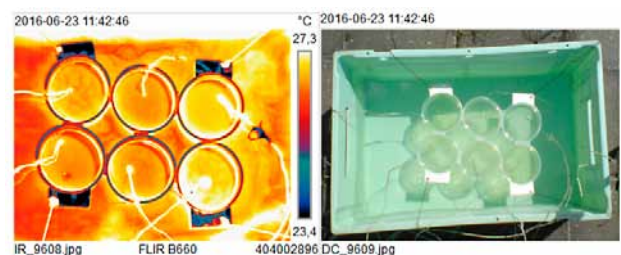


Fig. 14. Infrared (left) and digital (right) photos after two hours and a half from the beginning of the experiment

14 pav. Infraraudonųjų spindulių (kairė) ir skaitmeninė (dešinė) nuotraukos po 2:30 valandos nuo eksperimento pradžios

In the graph temperatures of layers with a diesel are increasing right after the shadow disappears. In this case, layers of diesel were in the shadow, from 11:37 till 11:41 (Fig. 15), and the photos were taken at 11:42. However, temperatures of the thickest layers of the diesel in the second row were lighter in the infrared photo than others. What is more, during every period with a shadow can be seen that temperatures of the thickest layers are decreasing less than temperatures in thinner layers.

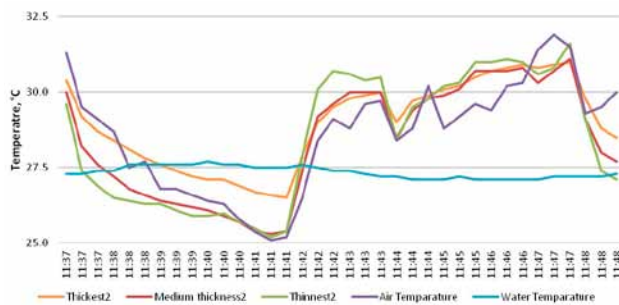


Fig. 15. Shadow effect on the temperatures of the air, water and layers of diesel (shadow from 11:37 till 11:41)

15 pav. Šešėlio poveikis oro, vandens ir dyzelio sluoksnių temperatūroms (šešėlis nuo 11:37 iki 11:41 val.)

In the figure 16 the differences between layers of diesel and water can be clearly seen. The thickest layers are the most noticeable in the infrared photo; also the second row of layers, which were affected by direct sunlight from the beginning of the experiment, shows more clear difference between the layers of diesel with different thickness.

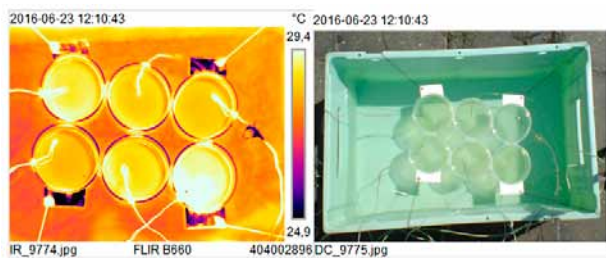


Fig. 16. Infrared (left) and digital (right) photos after three hours from the beginning of the experiment

16 pav. Infraraudonųjų spindulių (kairė) ir skaitmeninė (dešinė) nuotraukos po trijų valandų nuo eksperimento pradžios

Perhaps the clearest difference between the layers of diesel with different thickness and water can be seen in the figure 17. Colours of all surfaces are evenly distributed and water temperature is obviously lower than temperatures of the diesel layers (Fig. 18).

From the experimental results can be concluded that oil products (in this case diesel) can be detected with infrared camera. However, shadow/clouds have a significant effect

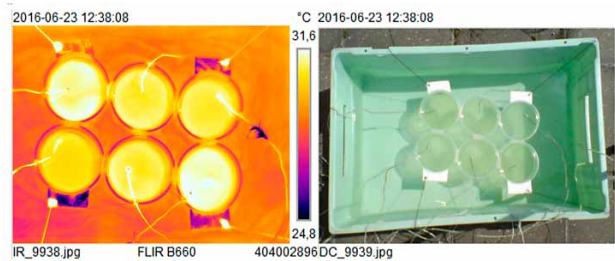


Fig. 17. Infrared (left) and digital (right) photos after three hours and a half from the beginning of the experiment

17 pav. Infraraudonųjų spindulių (kairė) ir skaitmeninė (dešinė) nuotraukos po 3:30 valandos nuo eksperimento pradžios

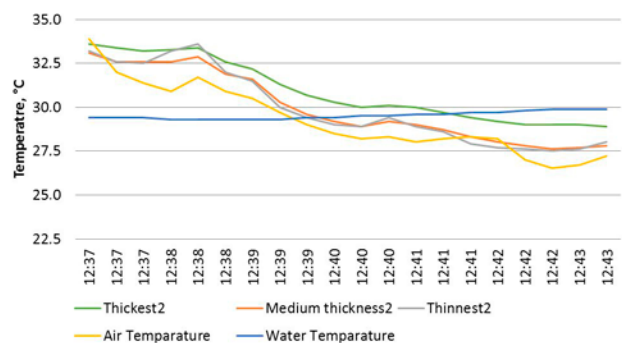


Fig. 18. Differences between temperatures of air, water and diesel layers in the second row

18 pav. Oro, vandens ir antros eilės dyzelio sluoksnių temperatūrų skirtumai

on efficiency of this remote sensing. For the clear difference in colours of surfaces with different temperatures direct sunlight is indispensable. As have been expected, the most obvious difference in colours was of the thickest layer of diesel and this difference was seen right after the beginning of the experiment. To see the difference between thinner layers and water was needed about 1–2 hours. Also, temperatures of diesel correlated with air temperature; still any connection between water temperature and diesel layers was not defined.

Conclusions

1. During experiment different thicknesses – 1, 2 and 3 mm – of diesel layers were detected using the thermal infrared FLIR camera.
2. In such type of experiments it's advisable use a container with water where layers of diesel with different thicknesses are formed and separated by 6 small transparent plastic rings.
3. Diesel can be detected with infrared camera, however, shadow/clouds have a significant effect on efficiency of this remote sensing method. For the clear difference in colours of surfaces with different temperatures direct sunlight is indispensable.

4. As have been expected, the most obvious difference in colours was of the thickest layer of diesel (3 mm) and this difference was seen right after the beginning of the experiment. To see the difference between thinner layers (1 and 2 mm thickness) and water was needed about 1–2 hours. Also, temperatures of layers with diesel correlated with air temperature; still any connection with temperature of water was not defined.

Padėkos

Dėkoju Civilinės inžinerijos mokslo centro Pastato energetinių ir mikroklimato sistemų laboratorijai kolektyvui už pagalbą atliekant eksperimentinius tyrimus.

References

- Fingas, M.; Brown, C. 2000. Review of oil spill remote sensing, *Marine Pollution Bulletin* 10(83): 199–208.
- Fingas, M. 2011. *Handbook of oil spill science and technology* [online], [cited 20 March 2017]. Elsevier, USA. ISBN: 978–1-85617–943–0. Available from Internet: www.elsevier.com
- Fingas, M. 2015. *Review of oil spill remote sensing technologies*. Spill Science, Edmonton, Alberta, Canada, vol. 9.
- Jha, M. N.; Levy, J.; Gao, Y. 2008. Advances in remote sensing for oil spill disaster management: state-of-the-art sensors technology for oil spill surveillance sensor, *Sensors for Disaster and Emergency Management Decision Making* 8(20): 236–255. <https://doi.org/10.3390/s8010236>
- Leifer, I.; Lehr, W. J.; Simecek-Beatty, D.; Bradley, E.; Clark, R.; Dennison, P.; Hu, Y.; Matheson, C.; Jones, C. E.; Holt, B.; Reif, M.; Dar A. Roberts, D. A.; Svejksky, J.; Swayze, G.; Wozencraft, J. 2012. State of the art satellite and airborne marine oil spill remote sensing: application to the BP Deepwater Horizon oil spill, *Remote Sensing of Environment* 124(25): 185–209. <https://doi.org/10.1016/j.rse.2012.03.024>
- Puestow, T.; Parsons, L.; Zakharov, I.; Cater, N.; Bobby, P.; Fuglem, M.; Parr, G.; Jayasiri, A.; Warren, S.; Warbanski, G. 2013. Oil spill detection and mapping in low visibility ice: surface remote sensing, *Arctic response technology: oil spill preparedness*. Final Report 5.1, vol. 84 p.

NAFTOS APTIKIMAS VANDENS PAVIRŠIUJE NAUDOJANT INFRARAUDONŲJŲ SPINDULIŲ KAMERA

K. Pilžis, V. Vaišis

Santrauka

Iš visų esamų nuotolinio aptikimo įrenginių infraraudonųjų spindulių sensoriai yra pigiausi ir plačiausiai naudojami. Šiame straipsnyje aprašytas eksperimentas buvo atliktas siekiant nustatyti, ar įmanoma aptikti naftos produktus ant vandens paviršiaus naudojant infraraudonųjų spindulių kamerą. Ši hipotezė buvo patvirtinta – storiausi naudoto naftos produkto sluoksniai turėjo didesnę temperatūrą nei vanduo. Taip pat buvo nustatyta, jog naftos produktų temperatūra tiesiogiai priklausė nuo oro temperatūros. Tačiau debesys turi labai didelę įtaką šio nuotolinio aptikimo metodui.

Reikšminiai žodžiai: naftos išsiliejimas, nuotolinis aptikimas, infraraudonieji sensoriai, šiluminė infraraudonųjų spindulių kamera.